WELDING RESEARCH

SUPPLEMENT TO THE *WELDING JOURNAL*, MAY 2000
Sponsored by the American Welding Society and the Welding Research Council

Partially Melted Zone in Aluminum Welds — Liquation Mechanism and Directional Solidification

Liquation is initiated eutectically and intensified by melting above the eutectic temperature, and the resultant liquid solidifies upward and toward the weld regardless of its position relative to the weld

BY C. HUANG AND S. KOU

ABSTRACT. Aluminum Alloy 2219 was welded by gas metal arc welding and the microstructure was examined in the partially melted zone (PMZ), which is a narrow region immediately outside the fusion zone. Extensive liquation was observed at three different locations: at large θ (Al_2Cu) particles, along grain boundaries (GBs) and at numerous isolated points within grains. Liquation was initiated at the eutectic temperature T_E, by the eutectic reaction $\alpha + \theta \rightarrow L_E$ and intensified by further melting, above T_E, of the α matrix surrounding the eutectic liquid (L_E). The microstructure of the liquated-and-solidified GB material is intriguing. First, the material consisted of a new GB of mostly thin, divorced eutectic and a eutectic-free strip of α immediately next to it. Second, within an individual grain, the strip was along the top and the side facing the weld. Third, with respect to the weld, the strip was always behind the new GB. These three characteristics point to an important phenomenon, that is, solidification of the liquated GB is directional — upward and toward the weld, as a result of the temperature gradients across the PMZ. A thin, brittle eutectic GB and a soft ductile α strip side by side are expected to be much weaker than a normal GB before welding.

C. HUANG and S. KOU are with the Department of Materials Science and Engineering, University of Wisconsin, Madison, Wis.

Introduction

Aluminum alloys tend to be susceptible to liquation along GBs during welding in a very narrow region immediately outside the fusion zone called the partially melted zone (PMZ) (Ref. 1). Grain boundary liquation in aluminum welds can have a serious consequence — it can make the PMZ susceptible to hot cracking (intergranular) during welding or ductility loss after welding. Liquated GBs are obviously weak and can be torn by tensile stresses induced during welding. Most studies on PMZ liquation in aluminum welds focused on the susceptibility to hot cracking during welding (Refs. 2–7). However, even if hot cracking is avoided during welding, the PMZ can still be susceptible to ductility loss after welding, as observed in tensile testing of the resultant welds (Refs. 8–10).

Unlike steels or nickel-based superalloys, little, if any, has been reported about the mechanism of welding-induced GB liquation in wrought aluminum alloys or about the GB microstructure after liquation. As aluminum alloys are gaining popularity (*e.g.*, in the auto industry) it is essential to better understand the welding of them.

KEY WORDS

Aluminum Alloys
Grain Boundaries
Gas Metal Arc Welding
Liquation
Eutectic
Partially Melted Zone (PMZ)

Experimental Procedure

The workpiece was Alloy 2219, a high-strength aluminum alloy often used for aerospace applications. The actual composition of the workpiece was Al-6.33%Cu-0.34%Mn-0.13%Fe-0.12%Zr-0.07%V-0.06%Si-0.04%Ti-0.02%Zn by weight. It was selected because it is essentially a binary alloy of Al-6.3wt-%Cu and its microstructure is, therefore, fairly easy to understand. The dimensions of the workpiece were 20 cm by 10 cm by 6.4 mm. It was welded in the as-received condition of T851. T8 stands for solution heat treating, cold working and followed by artificially aging, and T51 stands for stress relieving by stretching (Ref. 11).

Two bead-on-plate welds were made in the same workpiece by gas metal arc welding (GMAW), one perpendicular to the rolling direction and the other parallel. The welding parameters were 6.35 mm/s (15 in./min) welding speed, 25.5 V arc voltage, 190 A average current and argon shielding. The filler metal was an Alloy 2319 wire of 1.2-mm diameter. Its actual composition was Al-6.3%Cu-

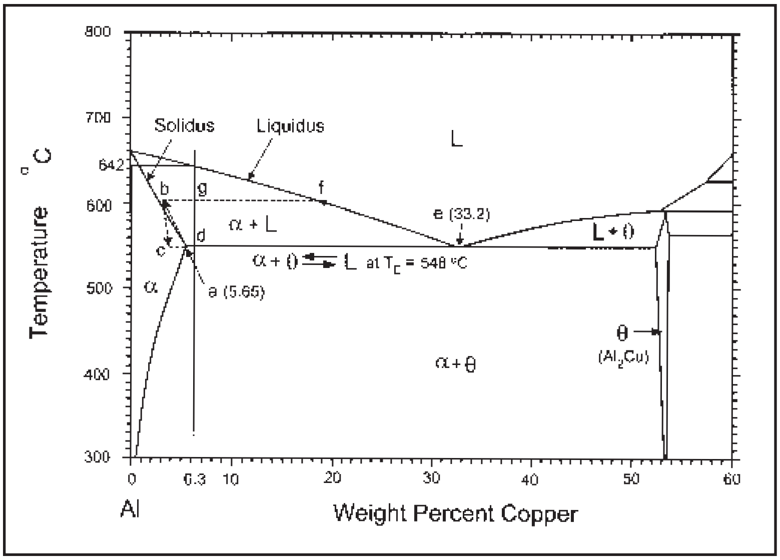

Fig. 1 — Al-Cu phase diagram (Ref. 12).

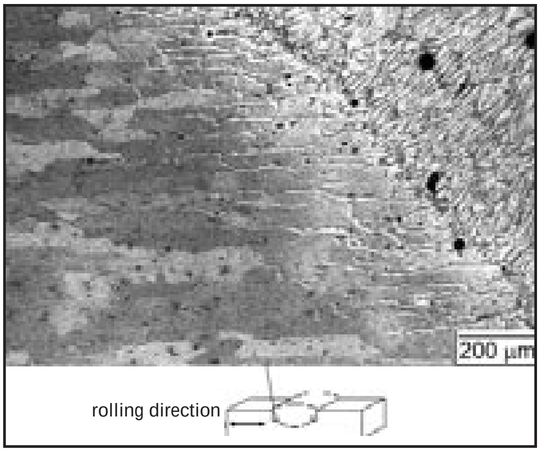

Fig. 2 — Partially melted zone in a GMA weld in 2219 aluminum alloy.

0.3%Mn-0.18%Zr-0.15%Ti-0.15%Fe-0.10%V-0.10%Si, which is higher in Zr and Ti than Alloy 2219. The wire feed speed was 13.5 cm/s (320 in./min).

After welding, the microstructure near the weld was examined by optical microscopy and by scanning electron microscopy with a secondary electron image. Several etching solutions, including Keller's, were tried, and the solution of 0.5 vol-% HF in water was found most satisfactory.

Results and Discussion

Overview of Partially Melted Zone

For convenience of discussion, the aluminum-rich portion of the Al-Cu phase diagram (Ref. 12) is shown in Fig. 1. The big gap between the solidus line and the liquidus line indicates the Cu content of the α phase (Al-rich solid) is much lower than that of the liquid. Since the 6.3% Cu content is about 20 times higher, or more than the content of any other alloying element, Alloy 2219 can be considered as a binary alloy of Al-6.3% Cu as an approximation.

Figure 2 is an optical micrograph showing an overview of the PMZ. The PMZ includes the region in which the GBs appear lighter in color. According to the Al-Cu phase diagram (Fig. 1), the liquation zone is in the narrow region immediately outside the fusion zone, where the maximum temperature experienced during welding ranges from the liquidus temperature of about 642°C on the fusion zone side (right) to the eutectic temperature of 548°C on the base metal side (left).

Base Metal

A scanning electron micrograph of the base metal is shown in Fig. 3A. Large particles are present both within grains and at GBs. Electron probe microanalysis (EPMA-WDS) indicates the Al/Cu weight ratio (*e.g.*, 53/46) of these particles is close to that of about 53/47 for θ (Al_2Cu) — Fig. 1. As an approximation, these particles will be considered as the θ phase even though they may contain very small amounts of other elements as well. As already mentioned, Alloy 2219 will be considered as a binary alloy of Al-6.3% Cu as an approximation. Figure 3A also shows several small θ particles within grains.

The small particles along the GBs are believed to be the θ phase also, although they are too small to be analyzed by EPMA. It is not clear why the GBs are not fully loaded with these small particles. The GBs do not look much different without etching.

The eutectic liquid during the terminal stage of solidification in ingot casting solidifies and forms large and small eutectic particles, along GBs and within grains. The solution heat-treating temperature for Alloy 2219 is 535°C (Ref. 13). From the phase diagram (Fig. 1), the base metal is expected to consist of a θ matrix plus additional undissolved θ (Al_2Cu) particles (Ref. 14). During solution heat treating of the ingot, the large eutectic islands decompose into large θ particles and α, which is connected to and hence indistinguishable from the α matrix. During rolling of the ingot into plates or sheets, some of the large θ particles are displaced or even fractured. Like the large eutectic particles, the GB eutectic also decomposes into θ particles and α, but this occurs much more rapidly in view of the smaller size and hence shorter distance required for diffusion. The presence of the large θ particles is an indication that the much smaller eutectic particles along GBs and within grains have already decomposed into θ and α.

Liquation at Large θ Particles

A scanning electron micrograph of the PMZ is shown in Fig. 3B. The two large particles within the grains do not look like the large θ particles within the grains of the base metal — Fig. 3A. Rather, their composite-like structure indicates they are eutectic. This suggests that in the PMZ the large θ particles within grains react with the surrounding α matrix to become liquid, which upon solidification forms large eutectic particles within grains. In other words, liquation occurs at large θ particles in the PMZ by the eutectic reaction $\alpha + \theta \rightarrow L_E$, where L_E is eutectic liquid.

Another scanning electron micrograph of the PMZ is shown in Fig. 3C. Large eutectic particles are present both within grains and at GBs, just like the large θ particles before welding — Fig. 3A. This again suggests that in the PMZ the large θ particles react eutectically with the surrounding α matrix to become liquid and form large eutectic particles upon solidification.

Constitutional liquation was first discovered by Pepe and Savage (Refs. 15, 16) in Maraging steel and later observed in Ni-based superalloys (Refs. 17–22) as well. This constitutional liquation and the liquation in the 2219 aluminum welds are both initiated at the eutectic temperature. They, however, differ from each other significantly in the following way. As pointed out by Pepe and Savage

(Refs. 15, 16), liquation is initiated before the solid-plus-liquid region of the phase diagram is reached during heating. It occurs only if the heating rate is rapid enough to prevent the second-phase particles (titanium sulfide) from dissolving in the single-phase region of the phase diagram. The liquation in the 2219 aluminum welds, however, is initiated simply because the solid-plus-liquid region of the phase diagram is reached during heating. It occurs even without a rapid heating rate.

Figure 4A shows an optical micrograph of the base metal, where the peak temperature during welding is well below the eutectic temperature T_E. Large θ particles (white) are present both within grains and at GBs. The distribution of large θ particles is not exactly uniform, and there are more of them in the area covered by this micrograph than in other areas of the base metal.

Figure 4B, shows an optical micrograph at the edge of the PMZ facing the base metal. The large particles on the left (θ) are still the θ phase, similar to those in Fig. 4A. The local temperature is, therefore, below T_E. The large particles (E) to the right of the large θ particles, however, are eutectic, and the local temperature is, therefore, above T_E. These large eutectic particles come from the large θ particles that have reacted with the surrounding α phase to form eutectic liquid. This eutectic liquid solidifies without changing its composition. Therefore, Fig. 4B represents the location where the peak temperature during welding is the eutectic temperature T_E. The arrows indicate the GBs that have become eutectic. The θ particles and one eutectic particle are enlarged in Fig. 4C to show the difference in the microstructure more clearly.

Figure 4D is another optical micrograph at T_E. The eutectic particles (E) are on the average larger than the θ particles (θ) in the same photo. In fact, a θ particle should expand after it reacts with the surrounding α phase to become eutectic liquid. Again, the arrows indicate the GBs that have become eutectic.

Figure 4E is an optical micrograph of the PMZ, where the peak temperature during welding is above the eutectic temperature T_E. Large eutectic particles are present within grains. This time they are surrounded essentially by a wide light-etching, eutectic-free material of the α phase. The large eutectic particles within grains shown previously in Fig. 3B and C are, in fact, similar in this respect except that the surrounding α phase does not appear any lighter in color under the scanning electron microscope. The presence of this α phase is explained below.

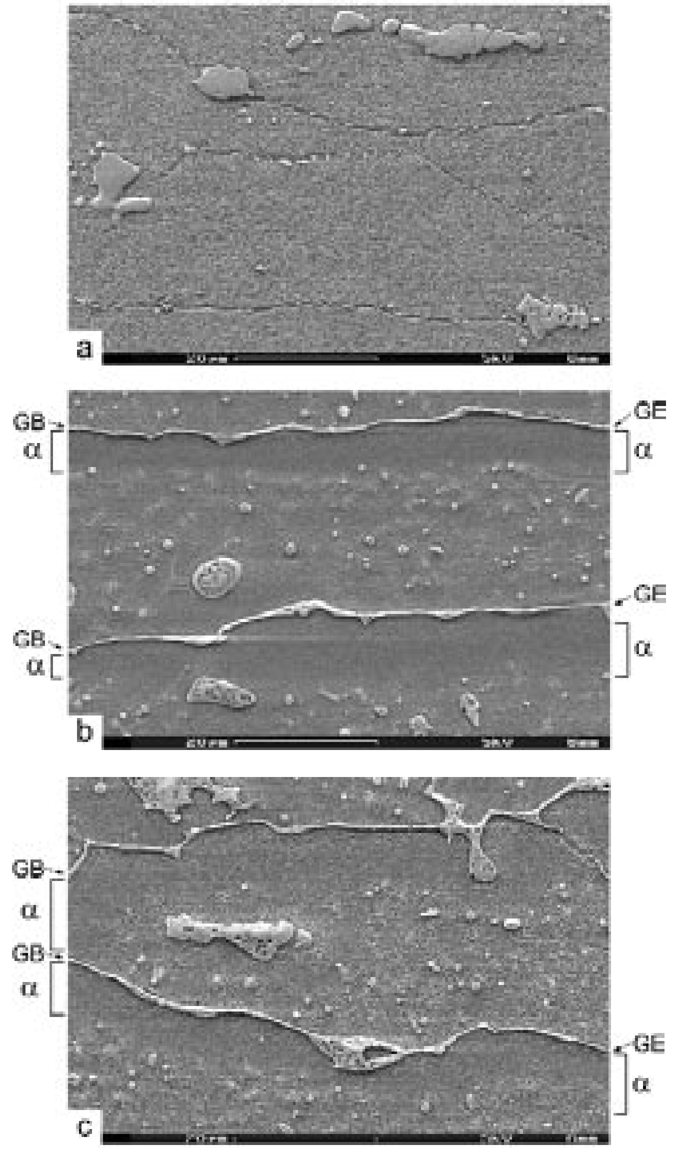

Fig. 3 — Scanning electron micrographs. A — Base metal; B and C — partially melted zone. Transverse cross section of weld made perpendicular to the rolling direction.

As already mentioned, when the peak temperature reaches the eutectic temperature T_E, the large θ particles react with the α phase and form eutectic liquid. Referring to the phase diagram in Fig. 1, the fraction of the liquid is $\overline{ad} / \overline{ae}$ according to the lever rule. When the peak temperature rises above T_E, the composition of the liquid changes along the liquidus line from point e at T_E to significantly above T_E, say, point f. The fraction of the liquid, $\overline{bg} / \overline{bf}$, is much greater than $\overline{ad} / \overline{ae}$. In other words, liquation is intensified by further melting of the α matrix surrounding the liquid. The liquid has now changed from eutectic to hypoeutectic in composition, and the large decrease in the Cu content of the liquid is achieved by melting the surrounding α phase of a much lower Cu content. Upon cooling, the hypoeutectic liquid solidifies initially as the α phase and finally as eutectic when T_E is reached. This is why the large eutectic particles are surrounded by the α phase. The fraction of the liquid that solidifies as eutectic, however, is expected to be greater than that based on the lever rule, that is, $\overline{ad} / \overline{ae}$. This is further explained as follows.

Since diffusion in solid is orders of magnitude slower than diffusion in liquid, the changes in the average composition of the α phase around the liquid are slower or less than those given by the solidus line. For instance, upon heating, the average composition of the α phase around the liquid can decrease from point a at T_E

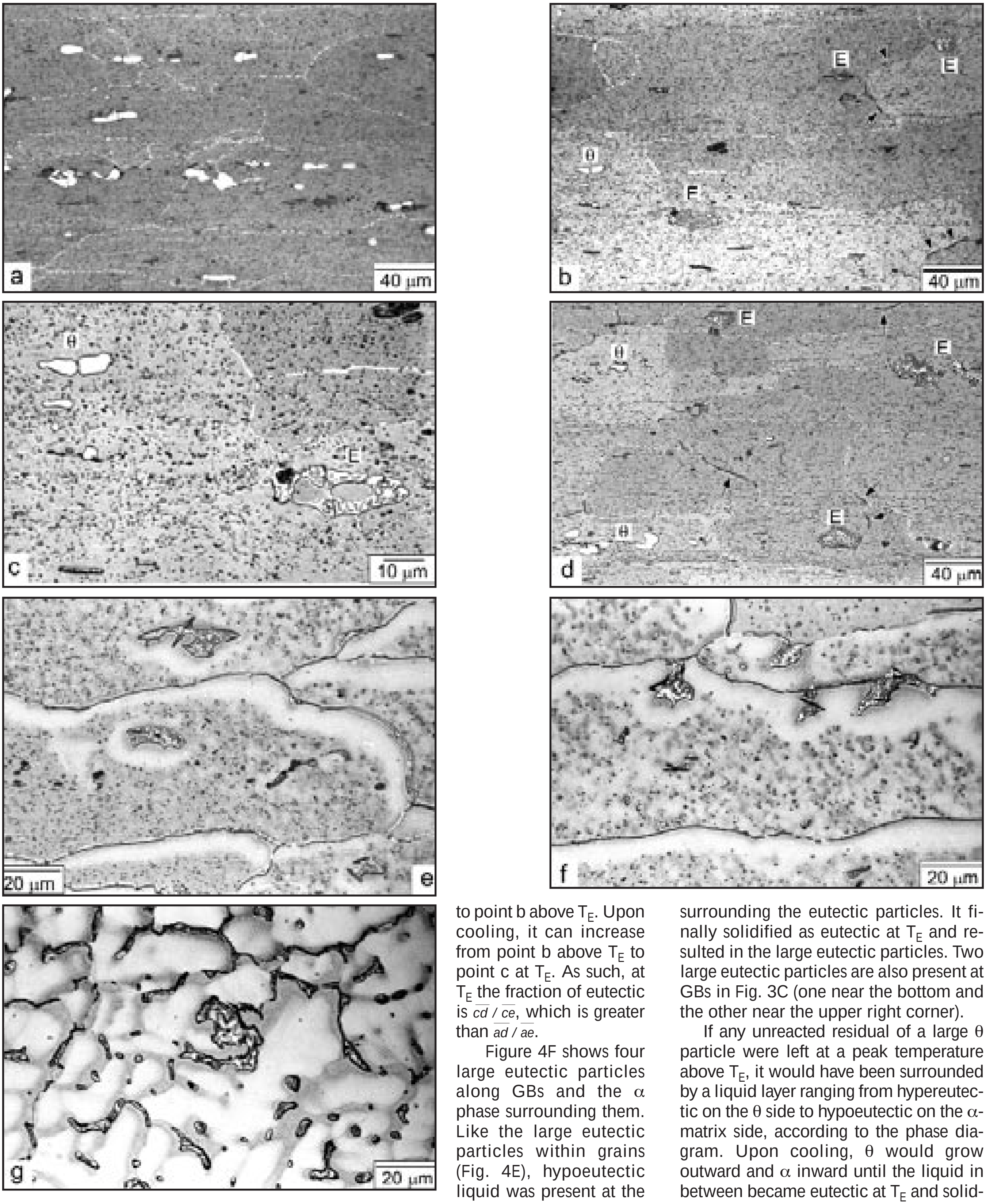

Fig. 4 — Optical micrographs. A — Base metal; B through D — edge of partially melted zone; E and F — partially melted zone; G — fusion zone. The arrows in B and D indicate the GBs that have become eutectic.

to point b above T_E. Upon cooling, it can increase from point b above T_E to point c at T_E. As such, at T_E the fraction of eutectic is $\overline{cd} / \overline{ce}$, which is greater than $\overline{ad} / \overline{ae}$.

Figure 4F shows four large eutectic particles along GBs and the α phase surrounding them. Like the large eutectic particles within grains (Fig. 4E), hypoeutectic liquid was present at the locations of these particles above T_E. Upon cooling, it solidified as the α phase above the eutectic temperature T_E and resulted in the light-etching, eutectic-free material surrounding the eutectic particles. It finally solidified as eutectic at T_E and resulted in the large eutectic particles. Two large eutectic particles are also present at GBs in Fig. 3C (one near the bottom and the other near the upper right corner).

If any unreacted residual of a large θ particle were left at a peak temperature above T_E, it would have been surrounded by a liquid layer ranging from hypereutectic on the θ side to hypoeutectic on the α-matrix side, according to the phase diagram. Upon cooling, θ would grow outward and α inward until the liquid in between became eutectic at T_E and solidified as such. The resultant structure would have been a θ core surrounded first by eutectic and then by Cu-depleted α. Such a structure with a θ core, however, does not appear to match that of large eutectic particles in the PMZ — Fig. 4E and F.

In summary, liquation at large θ particles in the PMZ appears to be initiated by the eutectic reaction $\alpha + \theta \rightarrow L_E$ at the eutectic temperature T_E, and intensified by further melting of the surrounding α phase above T_E.

Liquation at Grain Boundaries

Figures 3B and C show that, in the PMZ, GBs appear to be eutectic — divorced eutectic where the GB eutectic is thin and normal eutectic where it is thicker. In the former case, the α phase of the eutectic grows upon and is, therefore, indistinguishable from the primary α of the matrix, leaving θ alone visible at the GBs. In the latter, the GB eutectic shows the normal composite-like structure of (α + θ). The formation of GB eutectic is explained below.

As shown previously in Fig. 3A, small θ particles are present along GBs before welding. At the edge of the PMZ facing the base metal (Fig. 4B and D), the peak temperature during welding is T_E. Here, GB θ particles react eutectically with the surrounding α phase and form a thin liquid-eutectic GB film. Upon cooling, it solidifies as solid eutectic along GBs, as shown by the arrows in Fig. 4B and D. This GB eutectic is thin and hence more likely to be divorced than normal.

In the PMZ, however, the peak temperature during welding is above T_E. Here, the GBs are severely liquated, as shown in Fig. 4E. The GB eutectic appears to be mostly divorced, as mentioned previously (Fig. 3B and C). Adjacent to each GB is essentially a light-etching, eutectic-free strip of the α phase. Similar strips are, in fact, also present in Fig. 3B and C, except they do not look any lighter in color under the scanning electron microscope. The presence of an α strip along the GB is also evident in Fig. 4F. The reason for the presence of an α strip next to the GB eutectic is similar to that for the presence of the α phase surrounding the large eutectic particles within grains — Fig. 4E.

As already mentioned, when the peak temperature reaches the eutectic temperature T_E, the small θ particles along GBs react with the surrounding α phase and form a eutectic GB liquid. Referring again to the phase diagram in Fig. 1, when the peak temperature rises above T_E, the composition of the grain boundary liquid changes along the liquidus line from point e to, say, point f. Liquation intensifies as the fraction of the liquid rises significantly from $\overline{ad}/\overline{ae}$ to $\overline{bg}/\overline{bf}$. The large decrease in the Cu content of the GB liquid is achieved by melting the surrounding α phase of a much lower Cu content. Upon cooling, the hypoeutectic GB liquid solidifies initially as the α phase and finally as eutectic when T_E is reached. This explains why the GB eutectic is accompanied by a strip of the α phase.

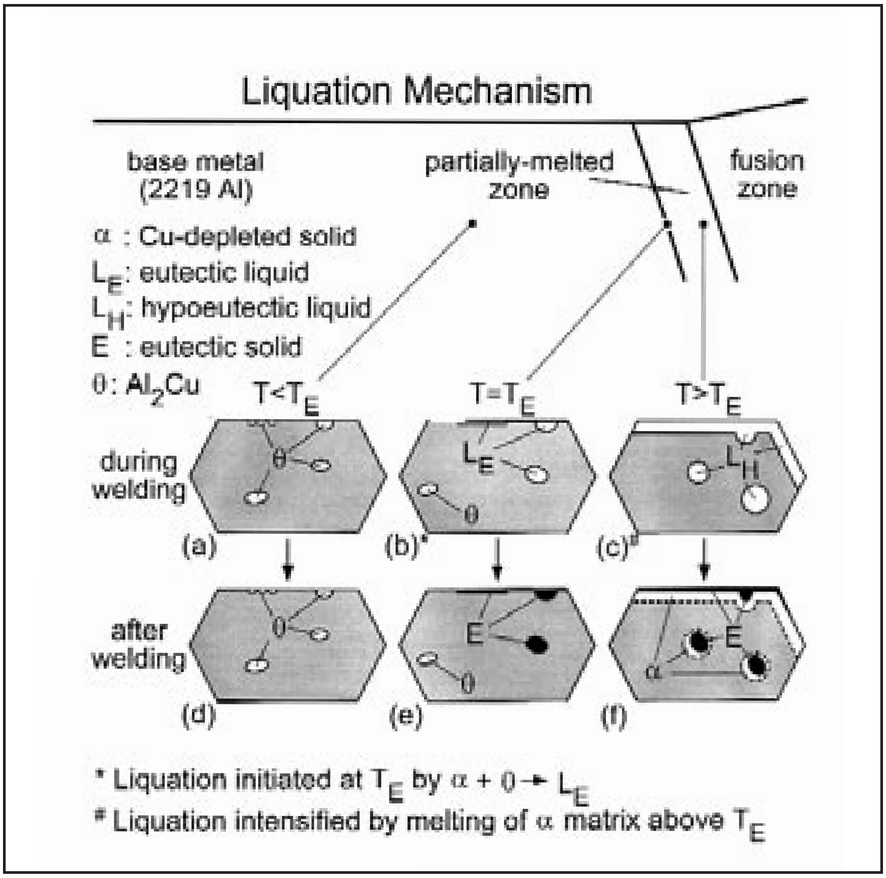

Fig. 5 — Schematic sketch showing the liquation mechanism in the partially melted zone.

One might suspect that Cu segregation to the GB by solid-state diffusion caused GB liquation. This liquation mechanism, however, raises the following questions. Why does Cu diffuse to the GB? Since the α strip appears on only one side of the GB (Figs. 3B, 3C, 4E and 4F), why does Cu diffuse to the GB from only one side? Furthermore, how can liquation within grains be explained?

Suppose within a narrow strip along the GB, Cu diffuses to the GB and causes it to melt. This solid-state diffusion leaves behind a Cu-depleted α strip along the GB (EPMA confirms Cu depletion in the α strip). Based on Figs. 3B, 3C, 4E and 4F, the α strips are about 10 µm (1×10^{-3} cm) wide. As an approximation, $x = Dt$, where x is the diffusion distance, D the diffusion coefficient and t the diffusion time. The diffusion coefficient for Cu in solid Al containing up to 3.5 wt-% Cu at around 600°C is about 1×10^{-8} cm^2/s (Refs. 14, 23). Based on these approximations, the time required for diffusion is 100 s. Obviously, this is far longer than the time the PMZ can possibly stay above the eutectic temperature during welding. Therefore, Cu segregation is not expected to be the mechanism for GB liquation.

It should be emphasized the equilibrium partition coefficient, k, for Cu in Al-6.3%Cu alloy is less than unity. Approximately, $k = 5.65/33.2 = 0.170$. Consequently, as the GB liquid solidifies, Cu is rejected into the liquid to cause severe Cu segregation. According to the PMZ micrographs shown in Figs. 3B, 3C, 4E and 4F, the GB liquid solidifies with the planar solidification mode. Initially, the solid has a very low Cu concentration. As solidification proceeds, however, Cu continues to be rejected into the liquid ahead of the planar solidification front. Eventually, the liquid becomes eutectic and solidifies as the eutectic GB. This is why there is a light-etching, Cu-depleted α strip right next to the eutectic GB. This strip is wide because, as already mentioned, the fraction of the liquid in the PMZ increases significantly with increasing temperature, *e.g.*, from $\overline{ad}/\overline{ae}$ at T_E to $\overline{bg}/\overline{bf}$ above T_E — Fig. 1. EPMA has confirmed severe Cu segregation from the α strip to the GB, as will be reported elsewhere.

The wide light-etching regions of Cu-

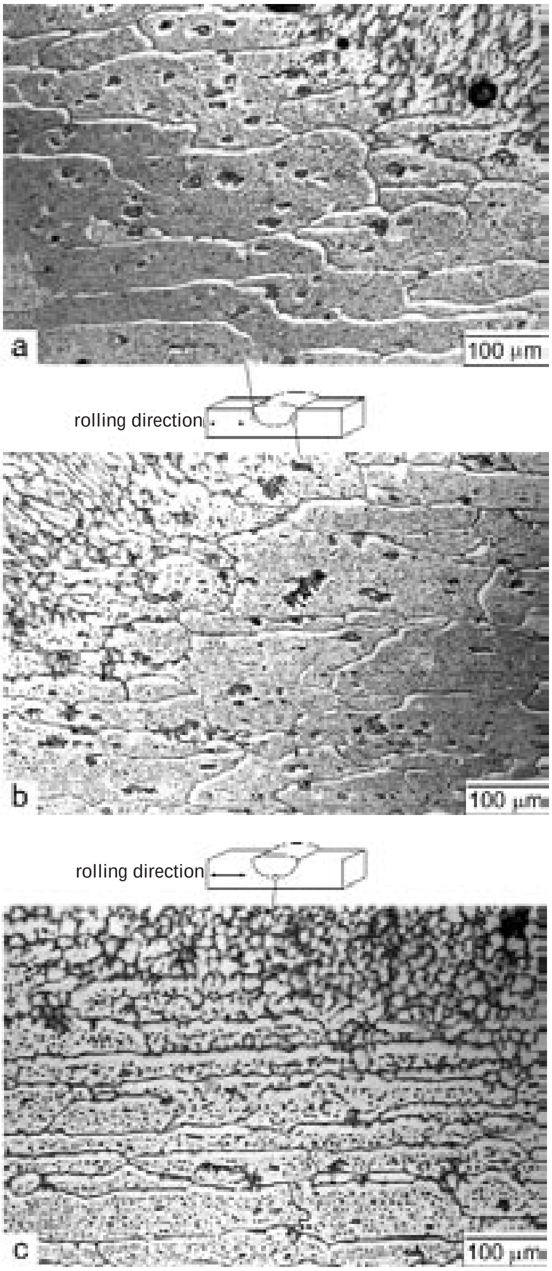

Fig. 6 — Optical micrographs of the transverse cross section of the partially melted zone of a weld made perpendicular to the rolling direction. A — Left; B — right; C — bottom.

depleted α both next to GBs and surrounding large eutectic particles represent the areas that were completely melted. This is not just an etching effect. Both the SEM and EPMA electron micrographs of an unetched PMZ show wide α regions similar to that of the light-etching, Cu-depleted regions in the optical micrographs of an etched PMZ. Furthermore, in the fusion zone, the regions next to the eutectic are also light etching, as shown in Fig. 4G. These regions were melted during welding.

Consider the case, if it does exist, that a certain portion of the GB does not have any small θ particles. The GB liquid can still reach here from adjacent areas of the same GB. Even if this does not happen, liquation can still occur when the local temperature rises above T_E to cause the α phase to melt. GB eutectic can still form during cooling, similar to path $\overline{bc}$ shown in Fig. 1.

In summary, referring to GBs along which small θ particles are present, GB liquation in the PMZ is initiated by the eutectic reaction $\alpha + \theta \rightarrow L_E$ at the eutectic temperature T_E and intensified by further melting of the adjacent α phase above T_E.

Figure 5 summarizes the constitutional liquation at large θ particles and along GBs in the PMZ of a 2219 aluminum weld.

Liquation at Numerous Isolated Points within Grains

Figures 4E and F show there are numerous small particles (round and dot-like) at isolated points within grains. These particles are believed to be eutectic and caused by liquation. The scanning electron micrographs in Fig. 3B and C also show such particles, but fewer. Presumably, only the larger ones are visible. Perhaps, with scanning electron microscopy, the color contrast of smaller particles against the α matrix is more limited.

Figures 4A through D show the presence of numerous small particles within grains in the base metal. These are likely to be the θ particles originating from the small eutectic particles within grains after casting. As mentioned previously, during the terminal stage of solidification in ingot casting, eutectic liquid is present in the numerous interdendritic spaces. During solution heat treating of the ingot, the interdendritic eutectic particles can decompose into θ and α. During rolling, the particles can be fractured and displaced, resulting in numerous small θ particles within grains. These small θ particles are not visible in Fig. 3A possibly because of the more limited color contrast in scanning electron microscopy again.

Upon heating to the eutectic temperature during welding, these θ particles react with the surrounding α matrix and form eutectic liquid, similar to the large θ particles and the small GB θ particles — Fig. 3A. Upon further heating to above the eutectic temperature, the liquid reduces its Cu content by melting the surrounding α phase of a much lower Cu content. Upon cooling, the hypoeutectic liquid first solidifies as α and finally as eutectic. Most of the resultant eutectic particles are expected to be divorced in view of their very small size. From Fig. 4E and F, almost all the round particles that are large enough to be seen more clearly appear to be divorced eutectic.

Directional Solidification

The microstructure of the liquated-and-solidified GB material has some interesting and significant characteristics that have not been reported previously. First, as already described, the material consists of a new GB and an α strip im-

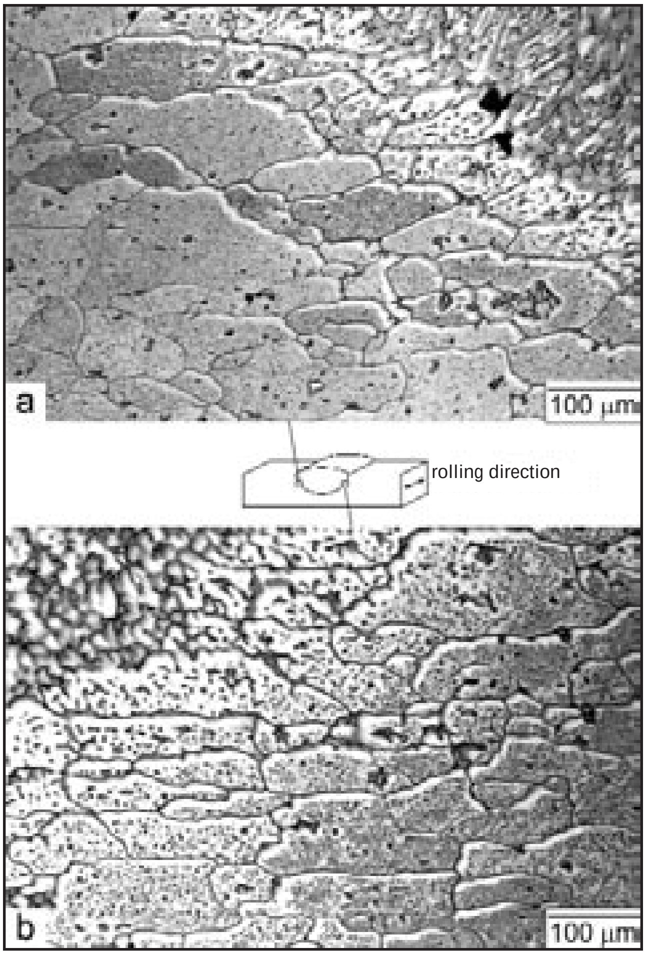

Fig. 7 — Optical micrographs of the transverse cross section of the partially melted zone of a weld made parallel to the rolling direction. A — Left; B — right.

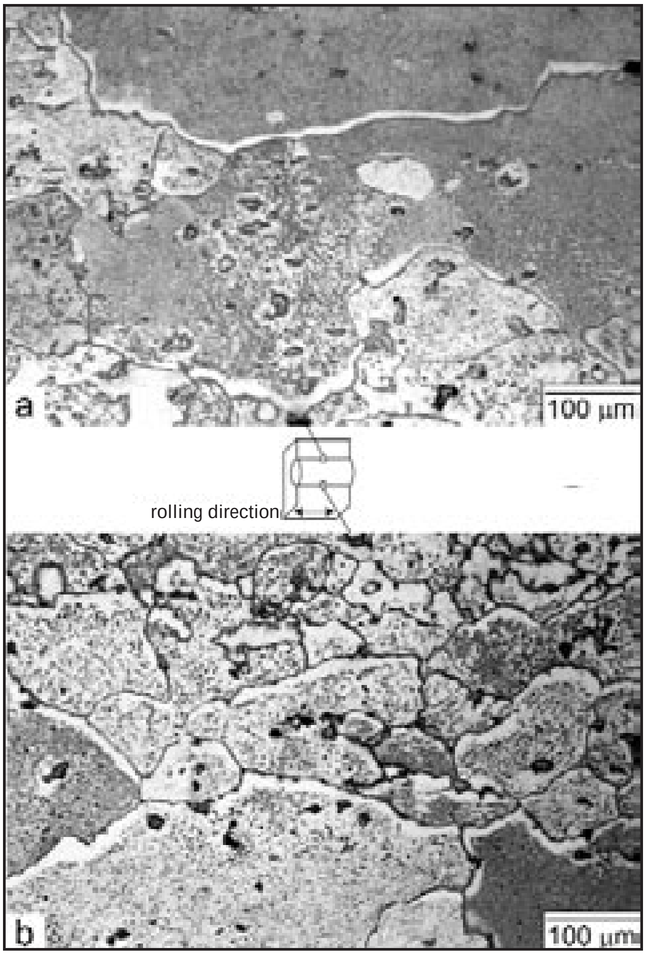

Fig. 8 — Optical micrographs showing top views of the partially melted zone of a weld made parallel to the rolling direction. A — One side; B — opposite side.

mediately next to it, the former being eutectic and the latter eutectic free. Second, within an individual grain the α strip is always along the top and the side facing the weld. Third, with respect to the weld, the α strip is always behind the new GB.

The second characteristic is evident in the weld made perpendicular to the rolling direction. Figure 6A is a PMZ micrograph on the left of the weld. Within a grain the α strip is present at the top and along the right side of the grain. Figure 6B, on the other hand, is a PMZ micrograph on the right of the weld. The α strip is at the top and along the left side of a grain. A PMZ micrograph at the bottom of the weld is shown in Fig. 6C. The α strip is at the top of a grain.

The second characteristic is also evident in the weld made parallel to the rolling direction, as shown in Figs. 7 and 8. In Fig. 7A, the strip is along the top and the right side of a grain, and in Fig. 7B it is along the top and the left side of a grain. In Fig. 8A, within an individual grain, the strip is along the side of the grain that faces the weld. The same is true in the micrograph in Fig. 8B.

The third characteristic is evident in the micrographs shown in Figs. 6–8. Within an individual grain, the light-etching strip is always on the side of the new GB that is farther away from the weld. In other words, with respect to the weld, the α strip is always behind the new GB.

The three characteristics of the microstructure of the liquated-and-solidified GB material are summarized in the schematic sketch in Fig. 9. These characteristics indicate the solidification of the liquated GB is directional. It solidifies upward and toward the weld — instead of inward from both grains it connects. To the best of the authors' knowledge, this directional solidification behavior of a GB liquid has not been reported previously. This behavior is the result of the significant temperature gradients across the PMZ of a weld.

From the heat flow point of view, the steeper the temperature gradients, the greater the tendency for a liquid to solidify in the direction of increasing temperature. Fourier's law of conduction can be written as $q = -k\nabla T$, where q is the heat flow rate per unit area, k the thermal conductivity and ∇T the temperature gradient (Ref. 24). The minus sign indicates heat is extracted in the opposite direction of the temperature gradient. The higher the temperature gradient, the faster heat is extracted to cause solidification in the direction increasing temperature.

Directional solidification is also evident from the large eutectic particles surrounded by the α phase. Figure 4E shows the three large eutectic particles are not at the center of the α phase. Rather, they shift upward and to the right toward the weld. The same is true with the many large eutectic particles in Fig. 6A.

Significance

Grain boundary liquation has long been known to cause hot cracking and ductility loss in the PMZ of aluminum welds. The α strip along the new GB is soft and ductile because it is not only eutectic free but also solute depleted. The

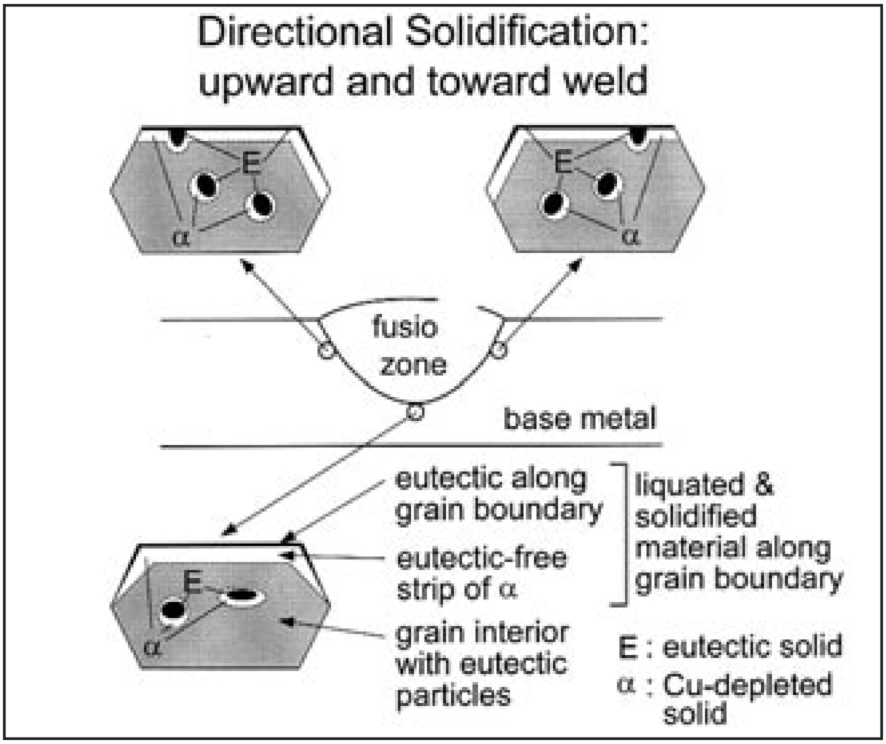

Fig. 9 — Schematic sketch illustrating directional solidification in the partially melted zone.

GB eutectic right next to it, however, is hard and brittle. Under tensile stresses the α strip is much better able to yield than the GB eutectic. (Due to space limitation, measurements of both hardness and solute segregation and fracture of GB eutectic under tension will be shown in a follow-up report.) A thin, hard, brittle, eutectic GB accompanied by a soft, ductile α strip is expected to be mechanically significantly inferior to a normal GB before welding. Aluminum alloys can lose ductility significantly in the PMZ, as mentioned previously (Refs. 8–10).

Conclusions

The GMA welds of 2219 aluminum alloy show extensive liquation can occur in the PMZ of aluminum welds. For Alloy 2219, liquation is initiated by the eutectic reaction $\alpha + \theta \rightarrow L_E$ at the eutectic temperature and intensified by melting of the surrounding α matrix above the eutectic temperature. Liquation occurs at large θ particles, along GBs and at numerous isolated points within grains. Liquation at large θ particles results in large eutectic particles. Grain boundary liquation results in new GBs that are more often divorced eutectic than normal eutectic. Liquation at isolated points within grains results in numerous small particles of divorced eutectic. The liquated GB solidifies upward and toward the weld under the influence of the temperature gradients across the PMZ. Such directional solidification results in a eutectic-free strip of the α phase right below and behind the eutectic GB.

Acknowledgments

This work was supported by the National Science Foundation under Grant No. DMR-9803589. The authors are grateful to Bruce Albrecht and Todd Holverson of Miller Electric Manufacturing Co., Appleton, Wis., for donating the welding equipment (including the Invision 456P power source, and XR-M wire feeder and gun) and for their technical assistance during this study. They also thank Walid Gabr-Rayan for conducting the welding experiments.

References

1. Kou, S. 1987. *Welding Metallurgy*. pp. 29–59, 239–262. New York, N.Y., John Wiley and Sons.
2. Robinson, I. B. 1978. *The Metallurgy of Aluminum Welding*. Pleasanton, Calif., Kaiser Aluminum Corp.
3. Gittos, N. F., and Scott, M. H. 1981. Heat-affected zone cracking of Al-Mg-Si alloys. *Welding Journal* 60(6): 95-s to 103-s.
4. Dudas, J. H., and Collins, F. R. 1966. Preventing weld cracks in high-strength aluminum alloys. *Welding Journal* 45(6): 241-s to 249-s.
5. Lippold, J. C., Nippes, E. F., and Savage, W. F. 1977. An investigation of hot cracking in 5083-0 aluminum alloy weldments. *Welding Journal* 56(6): 171-s to 178-s.
6. Metzger, G. E. 1967. Some mechanical properties of welds in 6061 aluminum alloy sheet. *Welding Journal* 46(10): 457-s to 469-s.
7. Steenbergen, J. E., and Thornton, H. R. 1970. Quantitative determination of the conditions for hot cracking during welding for aluminum alloys. *Welding Journal* 49(2): 61-s to 68-s.
8. Gibbs, F. E. 1966. Development of filler metals for welding Al-Zn-Mg Alloy 7039. *Welding Journal* 45(10): 445-s to 453-s.
9. Young, J. G. 1968. BWRA experience in the welding of aluminum-zinc-magnesium alloys. *Welding Journal* 47(10): 451-s to 461-s.
10. Arthur, J. B. 1955. Fusion welding of 24S-T3 aluminum alloy. *Welding Journal* 34(11): 558-s to 569-s.
11. The Aluminum Association. 1982. *Aluminum Standards and Data*. p. 15. Washington, D. C., The Aluminum Association.
12. *Binary Alloy phase Diagrams* 1: 106. 1986. Materials Park, Ohio, ASM International.
13. *Metals Handbook*, 9th Edition, Vol. 4, Heat treating, pp. 678–679. 1981. Materials Park, Ohio, ASM International.
14. Hatch, J. E. 1984. *Aluminum: Properties and Physical Metallurgy.* pp. 134–135, 140. Materials Park, Ohio, ASM International.
15. Pepe, J. J., and Savage, W. F. 1967. Effects of constitutional liquation in 18-Ni maraging steel weldment. *Welding Journal* 46(9): 411-s to 422-s.
16. Pepe, J. J., and Savage, W. F. 1970. Weld heat-affected zone of the 18Ni maraging steels. *Welding Journal* 49(12): 545-s to 553-s.
17. Owczarski, W. A., Duvall, D. S., and Sullivan, C. P. 1966. A model for heat-affected zone cracking in nickel-base superalloys. *Welding Journal* 45(4): 145-s to 155-s.
18. Duvall, D. S., and Owczarski, W. A. 1967. Further heat-affected zone studies in heat resistant nickel alloys. *Welding Journal* 46(9): 423-s to 432-s.
19. Savage, W. F., and Krantz, B. M. 1966. An investigation of hot cracking in Hastelloy X. *Welding Journal* 45(1): 13-s to 25-s.
20. Thompson, R. G., and Genculu, S. 1983. Microstructural evolution in the HAZ of Inconel 718 and correlation with the hot ductility test. *Welding Journal* 62(12): 337-s to 345-s.
21. Radhakrishnan, B., and Thompson, R. G. 1990. The kinetics of intergranular liquation in the HAZ of Alloy 718. *Recent Trends in Welding Science and Technology*. p. 637. ASM International, Materials Park, Ohio.
22. Radhakrishnan, B., and Thompson, R. G. 1993. Modeling of subsolidus liquation in the weld heat-affected zone. *International Trends in Welding Science and Technology*. p. 321, ASM International, Materials Park, Ohio.
23. Poirier, D. R., and Geiger, G. H. 1994. *Transport Phenomena in Materials Processing*. p. 432. The Minerals, Metals and Materials Society, Warrendale, Pa.
24. Kou, S. *Transport Phenomena and Materials Processing*. pp. 116–119. John Wiley and Sons, New York, N.Y.